Preparation and Properties of Heterocyclically Conjugated Poly(3-hexylthiophene)–Clay Nanocomposite Materials

Yuan-Hsiang Yu,[1,2] Chien-Chih Jen,[1] Hsiu-Ying Huang,[1] Pei-Chi Wu,[1] Chao-Cheng Huang,[1] Jui-Ming Yeh[1]

[1]*Department of Chemistry and Center for Nanotechnology at CYCU, Chung-Yuan Christian University, Chung Li, Taiwan 320, Republic of China*
[2]*Department of Electronic Engineering, Lan-Yan Institute of Technology, I-Lan 261, Taiwan, China*

Received 10 March 2003; accepted 15 July 2003

ABSTRACT: A series of heterocyclically conjugated polymer–clay nanocomposite (PCN) materials that consisted of organic poly(3-hexylthiophene) (P3HT) and inorganic montmorillonite (MMT) clay platelets were prepared by *in situ* oxidative polymerization with $FeCl_3$ as an oxidant. The as-synthesized PCN materials were characterized by Fourier transform infrared (FTIR) spectroscopy, wide-angle powder X-ray diffraction (WAXRD), and transmission electron microscopy (TEM). The effects of the material composition on the anticorrosion, gas barrier, thermal stability, flammability, mechanical strength, and electrical conductivity properties of the P3HT and PCN materials were studied by electrochemical corrosion measurements, gas-permeability analysis (GPA), thermogrametric analysis (TGA), limiting oxygen index (LOI) measurements, dynamic mechanical analysis (DMA), and a four-point probe technique, respectively. The molecular weights of extracted and bulk P3HT were determined by gel permeation chromatography (GPC) with THF as an eluant. © 2004 Wiley Periodicals, Inc. J Appl Polym Sci 91: 3438–3446, 2004

Key words: clay; nanocomposites; anticorrosion; conjugated

INTRODUCTION

Electronically conductive polymers, such as polyacetylene (polyene), polyaniline (polyaromatic hydrocarbon), and polythiophene (polyheterocycle), have received considerable attention lately because of their versatile promising technological applications. For example, organosoluble polythiophenes with long alkyl chain substituents in the 3-position of the thiophenes were found to display interesting anticorrosion properties.[1] Wei et al.[2] demonstrated the anticorrosion effect of polyaniline coatings through a series of electrochemical measurements on doped or undoped polyaniline-coated cold rolled steel (CRS) coupons. The use of poly(3-hexylthiophene)s (P3HTs) as a gas- or molecular-separation membrane was also reported.[3,4]

Smectite clay, such as montmorillonite (MMT), has attracted intense research interest for the preparation of polymer–clay nanocomposite (PCN) materials in the past decade because its lamellar elements exhibit high in-plane strength, stiffness, and a high aspect ratio.[5] Typically, the chemical structures of MMT consist of two fused silica tetrahedral sheets sandwiching an edge-shared octahedral sheet of either magnesium or aluminum hydroxide. The Na^+ and Ca^{+2} that reside in the interlayer regions could be replaced by organic cations such as alkylammonium ions by a cationic-exchange reaction to render the hydrophilic-layered silicate organophilic. Smectite clays in the polymer matrix were found to boost the gas-barrier,[6–8] thermal stability,[9] mechanical strength,[10] and fire-retardant[11] properties of polymers. In the past decade, many research groups have devoted efforts to the preparation and properties of nanocomposites of conductive polymers with various layered materials.[12–18] Recently, we[19] reported the enhanced anticorrosive properties of polyaniline–clay nanocomposite coatings on CRS coupons relative to bulk polyaniline on the basis of a series of electrochemical measurements in saline. Similar results were also found in PMMA–clay[20] and PEA–clay[21] nanocomposite materials.

In this article, we present the preparation and properties of a series of heterocyclically conjugated P3HT–clay nanocomposite materials via an *in situ* oxidative polymerization. The as-synthesized PCN materials were characterized by FTIR spectroscopy, wide-angle powder X-ray diffraction (WAXRD), and TEM. The effects of the material composition on the anticorrosion, gas-barrier, thermal stability, flammability, mechanical strength, and electrical conductivity properties of P3HT and PCN materials were studied by electrochemical corrosion measurements, gas permeability analysis (GPA), thermogravimetric analysis (TGA), limiting oxygen index (LOI) measurements,

Correspondence to: J.-M. Yeh (juiming@cycu.edu.tw).
Contract grant sponsor: NSC; contract grant number: 92-2113-M-033-004.

dynamic mechanical analysis (DMA), and a four-point probe technique, respectively. Molecular weights of extracted and bulk P3HT were determined by gel permeation chromatography (GPC) with tetrahydrofuran (THF) as an eluant.

EXPERIMENTAL

Chemicals and instrumentation

3-Hexylthiophene (99%, Aldrich, Milwaukee, WI) and anhydrous $FeCl_3$ (Lancaster, Morecambe, England) was used directly without further purification. Chloroform (99.99%, Assay, New Jersey) was employed as solvent and dried prior to use. THF (Fisher Scientific, New Jersey) was employed as an eluant for GPC measurements. Methyl alcohol (99.99%, Tedia, New Jersey) was used as a solvent for precipitating and extracting the polymers. The MMT clay used with a CEC value of 114 mequiv/100 g and the formula of $Ca^{+}_{0.084}Na_{0.143}Al_{1.69}Mg_{0.31}Si_4O_{10}(OH)_2 \cdot 2H_2O$ was provided by the Industrial Technology Research Institute (ITRI) (Hsinchu, Taiwan). Tetradecyltrimethylammonium chloride (≥98%, Fluka) was employed as an intercalating agent.

A WAXRD study of the samples was carried out using a Rigaku D/MAX-3C OD-2988N X-ray diffractometer with a cooper target and Ni filter at a scanning rate of 4°/min. The samples for the transmission electron microscopy (TEM) study were first prepared by putting a powder of the PCN materials into low-viscosity embedding media capsules with four ingredients (ERL4206 5.0 g, DER736 3.0 g, NSA 13.0 g, and DMAE 0.15 g) and by curing the media at 80°C for 12 h in a vacuum oven. Then, the cured capsules containing the PCN materials were microtomed with a Leica Ultracut Uct into 90-nm-thick slices. Subsequently, one layer of carbon about 10 nm thick was deposited on these slices on 100-mesh copper nets for TEM observation on a JEOL-200FX with an acceleration voltage of 120 kV. FTIR spectra were recorded on pressed KBr pellets using a Bio-Rad FTS-7 FTIR spectrometer. The molecular weight of the polymer extracted from all the composite samples as well as bulk P3HT was determined on a Waters GPC Model 2 II equipped with a Model 590 programmable solvent-delivery module, a differential refractometer detector, and a Styragel HT column with THF as the eluant and monodispersed polystyrenes as calibration standards.

Electrochemical corrosion measurements were performed on a VoltaLab Model 21 and VoltaLab Model 40 potentiostat/galvanostat in a standard corrosion cell. The dynamic mechanical analyses for the sample membranes were carried out from −50 to 100°C with a Perkin–Elmer DMA 7e analyzer at a heating rate of 5°C at a fixed frequency of 1 Hz. A Perkin–Elmer thermal analysis system equipped with a Model 7/DX TGA was employed for the thermal analyses under an air flow. The programmed heating rate was 20°C/min in most cases. Conductivity measurements were made on a four-point probe connected to a Keithley 2400 voltmeter constant-current source system. The samples were, in the form of compacted disk pellets, 12.6 mm in diameter and ~1 mm thick. Three measurements were made on each of the duplicate samples. LOI values were measured on an United States Testing 8100 flame meter by a modified method that has been investigated in the literature.[22,23] The percentage in the O_2/N_2 mixture deemed sufficient to sustain the flame was taken as the LOI.

Synthesis of P3HT

$FeCl_3$-doped P3HTs were synthesized by a one-step oxidative polymerization in the presence of anhydrous $FeCl_3$ in dry chloroform, according to the method reported by Hotta et al.[24] and Kang et al.[25] A mixture of $FeCl_3$ (5.84 g, 36 mmol) and dry chloroform (100 mL) was placed in a reaction flask under a dry nitrogen atmosphere and was vigorously magnetically stirred overnight at room temperature; the 3-hexylthiophene monomer (2.02 g, 12 mmol) was then introduced dropwise into the oxidant solution under magnetic stirring for another 24 h. The reaction mixture was subsequently poured into a large excess amount of methanol (300 mL) to precipitate the $FeCl_3$-doped P3HT. The as-synthesized product was then treated by Soxhlet extraction to remove $FeCl_3$. The typical yield for the undoped form of P3HT was about 92%.

Preparation of organophilic clay[19–21]

Organophilic clay was prepared by a cation-exchange reaction between the sodium cations of MMT clay and alkylammonium ions of an intercalating agent, tetradecyltrimethylammonium chloride. Typically, MMT (10 g) with a CEC value of 114 mequiv/100 g (ITRI) was stirred in 500 mL distilled water (beaker A) at room temperature overnight. A separate solution contained 4 g of the intercalating agent in another 100 mL of distilled water (beaker B) was magnetically stirred, followed by adding a 1*M* HCl aqueous solution to adjust the pH value to the range of 3–4. After stirring for 1 h, the tetradecyltrimethylammonium chloride solution (beaker B) was added at a rate of approximately 10 mL/min with vigorous stirring to the MMT suspension (beaker A). After mixing, the mixture was stirred overnight at room temperature. The organophilic clay was recovered by ultracentrifugating (7500 rpm, 30 min) and filtering the solution in a Buchner funnel. The procedure of washing (with distilled water) and filtering was repeated five times to remove any excess of ammonium ions.

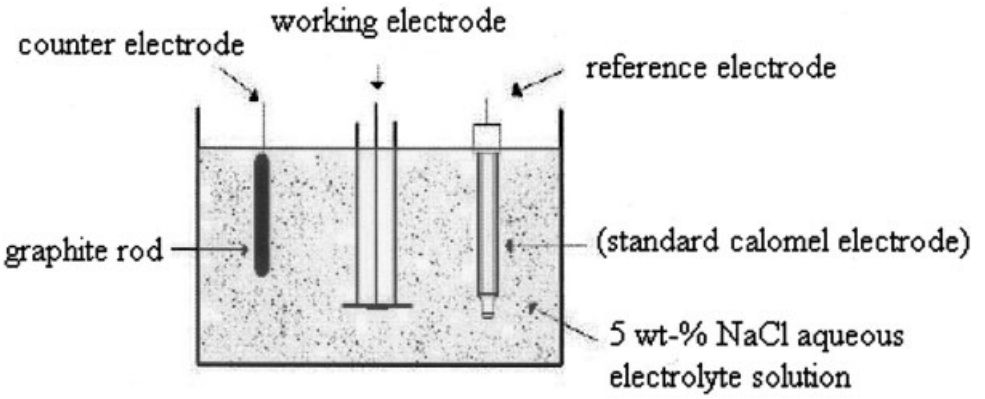

Scheme 1

Preparation of P3HT–clay nanocomposite materials

As a typical procedure to prepare nanocomposite materials incorporated with 1 wt % clay is described as follows: $FeCl_3$ (5.987 g, 36 mmol) and 50 mL of dry chloroform were mixed in the reaction flask (flask A) under a dry nitrogen atmosphere and magnetically stirred at room temperature. On the other hand, 0.021 g of organophilic clay was suspended into dry chloroform in another reaction flask (flask B) under a N_2 atmosphere and magnetically stirred for 24 h. The 3-hexylthiophene monomers (2.03 g, 12 mmol) were introduced into flask B under magnetic stirring for another 24 h. The solution in flask A was then added to flask B under a N_2 atmosphere. After mixing, the combined solution was allowed to react at room temperature overnight. The as-synthesized products were precipitated from 300 mL of methanol and followed by suction under a vacuum.

Preparation of coatings and electrochemical measurements

As a typical procedure to prepare sample-coated coupons for corrosion protection measurements, 1 wt % solutions of P3HT and PCN fine powder in chloroform were cast dropwise onto the CRS coupons (1 × 1 cm) followed by drying in air for 2 h at 100°C to give ~20-μm-thick coatings, measured by a digimatic micrometer (Mitutoyo). The coated and uncoated coupons were mounted onto the working electrode so that only the coated side of the coupon was in direct contact with the electrolyte. The edges of the coupons were sealed with superfast epoxy cement (SPAR®). Electrochemical corrosion measurements were performed on a VoltaLab 21 potentiostat/galvanostat in a standard corrosion test cell equipped with two graphite rods (diameter: 6.15 mm), counter-electrodes, a saturated calomel reference electrode (SCE), and the above-mentioned working electrode, as shown in Scheme 1. The potentials were reported in reference to SCE. All the electrochemical measurements were made at room temperature and repeated at least three times. The electrolyte was a NaCl (5 wt %) aqueous solution. The open-circuit potential (OCP) at the equilibrium state of the system was recorded as the corrosion potential (E_{corr} in volts versus SCE). The polarization resistance (R_p in Ω/cm^2) was measured by sweeping the applied potential from 20 mV below to 20 mV above the E_{corr} at a scan rate of 500 mV/min and recording the corresponding current change. The R_p value was obtained from the slope of the potential–current plot. Tafel plots were obtained by a scanning potential from 250 mV below to 250 mV above the E_{corr} at a scan rate of 500 mV/min. The corrosion current (i_{corr}) of the material-coated CRS was determined by superimposing a straight line along the linear portion of the cathodic or anodic curve and extrapolating it through E_{corr}. The corrosion rate [R_{corr}, in milli-inches per year (MPY)] was calculated from the following equation:

$$R_{corr}(\text{MPY}) = [0.13 i_{corr}(\text{E.W.})]/[\text{A d}] \quad (1)$$

where E.W. is the equivalent weight (in g/equiv); A, the area (in cm^2); and d, the density (in g/cm^3). A VoltaLab Model 40 potentiostat/galvanostat was used to perform the ac impedance spectroscopy measurements. Voltamaster 4 (Version 2.0), supplied by Radiometer Copenhagen, was employed as software. Impedance measurements were performed in the frequency range of 100 K to 100 mHz. The working electrode was first maintained in the test environment for 30 min before the impedance run. This procedure served to put the electrode in a reproducible initial state and ensure that no blistering occurred during the conditioning period. All experiments were operated at a laboratory temperature of 25 ± 1°C. All raw data were repeated at least three times to ensure reproducibility and statistical significance.

TABLE I
Relations of the Composition of P3HT–MMT Clay Nonocomposite Materials with the E_{corr}, R_p, i_{corr}, R_{corr}, Permeability, Char Yield, LOI Value, Electrical Conductivity, and Product Yield as Measured from Electrochemical Corrosion Measurements, Gas-permeability Measurements, TGA, LOI Measurements, and Four-probe Measurements

	Feed composition (wt %)		Electrochemical measurements[a]			Gas permeability[b]					
Compound code	P3HT	MMT	E_{corr} (mV)	R_p (KΩ cm^2)	i_{corr} (μA/cm^2)	R_{corr} (MPY)	P (barrers)	Yield (%)	Char yield[c] (wt %)	LOI[d] value	Conductivity[e] log(σ) (s/cm)
Bare	—	—	−620	0.68	46.14	89.5	—	—	—	—	—
P3HT	100	0	−580	10.68	4.52	8.8	23.13	92.5	3.40	27.0	−4.59
CL01	99	1	−536	86.83	0.67	1.3	21.42	81.4	35.62	29.0	−8.52
CL03	97	3	−535	196.75	0.21	0.4	19.47	79.4	37.14	30.5	—
CL05	95	5	−526	204.59	0.17	0.3	18.03	62.6	38.32	32.4	−8.40
CL07	93	7	−463	704.77	0.06	0.1	17.28	84.0	39.96	33.5	—
CL10	90	10	−460	1340.00	0.05	0.1	15.78	75.3	41.15	36.0	−8.40

[a] As measured from electrochemical measurements. Saturated calomel electrode was employed as reference electrode.
[b] As measured from gas-permeability measurements.
[c] As measured from TGA measurements.
[d] As measured from LOI measurements.
[e] As measured from four-probe measurements.

Preparation of membranes and gas-barrier properties measurements

As a representative procedure to manufacture membranes for gas-barrier property measurements, a dedoped form of P3HT or PCN materials (0.3 g) was first dissolved in 10 mL chloroform under magnetic stirring at room temperature for 4 h. The solution was then cast onto a substrate (e.g., a microscope glass slide). The solvent was allowed to evaporate at 40°C under the hood for 24 h. The membranes were lifted from the glass substrates by soaking in distilled water for ~1 h and dried under a vacuum for 24 h at room temperature. Gas-barrier properties for sample membranes were determined by air transmission of nanocomposite membranes according to ASTM standard E 96. A Yanagimoto Co., Ltd., gas-permeability measuring apparatus (Model GTR 10) was employed to perform the permeation experiment of air. The rate of transmission of air was measured by gas chromatography. The air permeability was calculated from the rate.

Molecular weights of bulk and extracted P3HTs

A reverse cationic-exchange reaction was employed to separate bound P3HT from the inorganic component in the PCN materials. As a typical extraction procedure, 2 g of fine powder of as-synthesized PCN materials was dissolved in ~100 mL of methanol (beaker A). Separately, a 10 mL stock solution of 1 wt % $LiCl_{(s)}$ in methanol was prepared (beaker B). Both beakers were under vigorous magnetic stirring for 3–4 h at room temperature. After combining the contents of the two beakers, the mixture was stirred for additional 24 h followed by Soxhlet extraction at 85–90°C for 48 h. The extract solution was evaporated on a rotavapor under a reduced pressure at 50°C to yield P3HT fine powders. Molecular weights of both extracted and bulk P3HT were determined by GPC analyses with THF as an eluant.

RESULTS AND DISCUSSION

Poly(3-alkylthiophene)s, heterocyclically conjugated organosoluble polymers, recently have attracted much interest because of their high level of solution and melt processibility. P3HT is one of the most studied poly(3-alkylthiophene)s and is known as a semicrystalline polymer. On the other hand, MMT is a clay mineral containing stacked silicate sheets measuring ~10 Å in thickness and ~2000 Å in length.[26] It possesss a high aspect ratio and a platey morphology. MMT has a high swelling capacity, which is essential for efficient intercalation of the polymer, and is composed of stacked silicate sheets that offer enhanced chemical and physical properties.

To prepare the PCN materials, organophilic clay was first prepared by a cationic-exchange reaction between the sodium cations of clay and alkylammonium ions of the intercalating agent. Organic 3-hexylthiophene monomers were subsequently intercalated into the interlayer regions of the organophilic clay hosts, followed by a one-step oxidative polymerization. The composition of the PCN materials was varied from 0 to 10 wt % of clay with respect to the P3HT content as summarized in Table I.

Characterization

In the FTIR spectra of the PCN materials, the vibrational bands of P3HT were shown at 776 cm^{-1} (C—S),

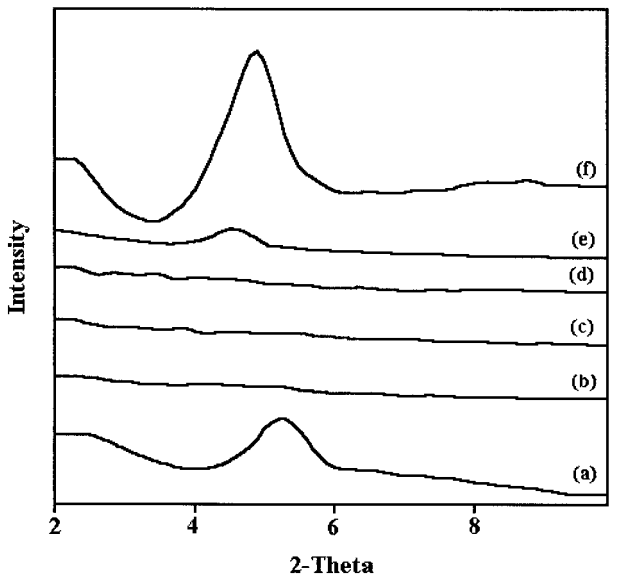

Figure 1 WAXRD diffraction patterns for (a) P3HT, (b) CL01, (c) CL03, (d) CL05, (e) CL10, and (f) organophilic clay.

2852 cm^{-1} (—CH_2—), and 2923 cm^{-1} (—CH_3), and those of MMT clay were shown around 1100 cm^{-1} (Si—O), 500 cm^{-1} (Al—O), and 400 cm^{-1} (Mg—O).[19–21] As the MMT clay loading increased, the characteristic vibrational peak intensity of MMT clay became stronger. Figure 1 shows the XRD patterns of organophilic clay, P3HT, and PCN materials. The crystalline behavior of bulk P3HT is observed in curve (a) with an intense peak appearing near $2\theta = 5.4°$ (d spacing = 16.4 Å). The diffraction peak of organophilic clay shown in curve (f) is $2\theta = 4.75°$, corresponding to a d spacing of 18.6 Å. As shown in curves (b)–(d) of Figure 1, the powder XRD patterns of the PCN materials did not show any diffraction peak in $2\theta = 2–10°$, indicating the possibility of having exfoliated silicate layers of organophilic clay dispersed in the P3HT matrix and the dispersed nanolayers of MMT clay in the polymer matrix would change the crystalline behavior of P3HT. When the amount of organoclay increased to 10%, there was a small peak appearing at $2\theta = 4.45°$, corresponding a d spacing of 22 Å, which implied that there was a small amount of organoclay that cannot be exfoliated in the P3HT and that existed in the form of an intercalated layer structure as a result of swelling by the P3HT molecules. That the crystalline behavior of the P3HT–clay nanocomposite materials became amorphous might be attributed mainly to that the molecular weight decreased when prepared by *in situ* polymerization as in our previous studies in PVA–clay nanocomposite materials.[27]

In Figure 2, a transmission electron microscopy micrograph of the PCN materials with 10 wt % clay loading shows that the nanocomposite material exhibits a mixed nanomorphology. Individual silicate layers, along two- and three-layer stacks, were found to be well dispersed in the polymer matrix. Some larger intercalated tactoids were also observed.

Anticorrosion properties of coatings

The corrosion protection performance of PCN materials on CRS coupons was evaluated through the values of the corrosion potential (E_{corr}), polarization resistance (R_p), corrosion current (i_{corr}), and corrosion rate (R_{corr}), as shown in Table I. The CRS coupon coated with undoped P3HT exhibited a higher E_{corr} value than that of the uncoated CRS. However, it showed a much lower E_{corr} value than that of the specimen coated with PCN materials. For example, the CL01-coated CRS exhibited a high corrosion potential of about −536 mV at 30 min. Even after 5-h measurement, the potential remained constant at about −540 mV. Such an E_{corr} value implied that the CL01-coated CRS was noble toward the electrochemical corrosion relative to the undoped P3HT. The CL01-coated CRS showed a polarization resistance (R_p) value of 8.68×10^4 Ω/cm^2 in 5 wt % NaCl, which was about 2 orders of magnitude greater than that of the uncoated CRS. The Tafel plots for (a) bare, (b) P3HT-coated, (c) CL05-coated, and (d) CL10-coated CRS are shown in Figure 3. The corrosion current (i_{corr}) of CL01-coated CRS was about 0.67 $\mu A/cm^2$, which corresponds to a

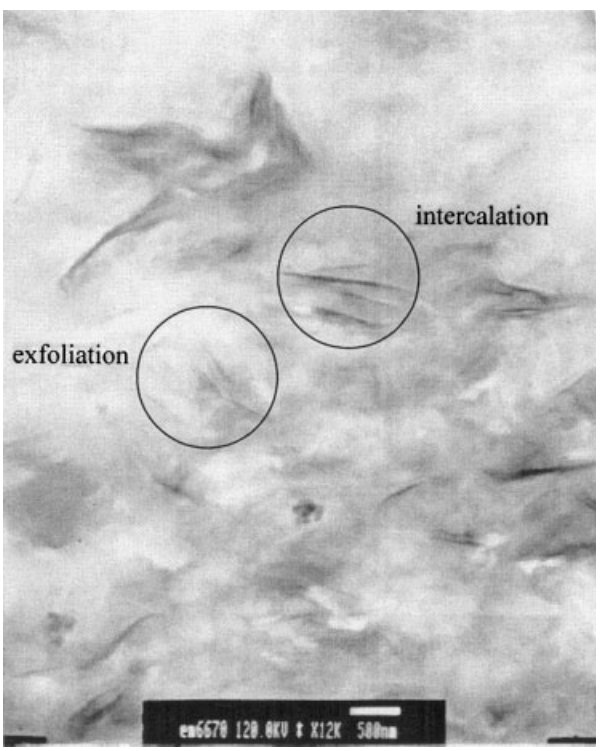

Figure 2 TEM micrograph of CL10 at 12 K magnification.

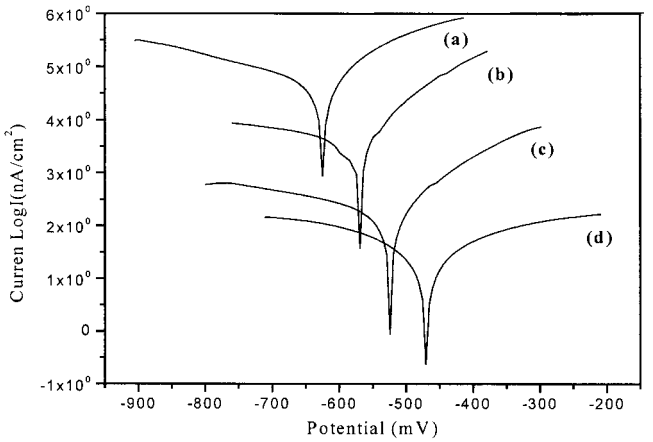

Figure 3 Tafel plots for (a) bare, (b) P3HT-coated, (c) CL05-coated, and (d) CL10-coated CRS measured in 5 wt % NaCl aqueous solution.

corrosion rate (R_{corr}) of about 1.30 MPY, as summarized in Table I.

Electrochemical impedance spectroscopy (EIS) was also used to examine the activity difference between the CRS surface after treatment of P3HT and the PCN materials. To this end, two samples were prepared. A series of samples denoted with (a) and (b) were CRS-coated by P3HT and CL05. The corrosion of these samples in a 5 wt % NaCl aqueous electrolyte for 30 min was followed by EIS. Figure 4 shows Nyquist plots of the three samples. The charge-transfer resistances of samples (a) and (b) that could be determined by the intersection of the low-frequency end of the semicircle arc with the real axis were 76.5 and 305 KΩ cm^2, respectively. The results obviously show that the sample incorporated with clay nanolayers had a better anticorrosive performance. Visual observation for the

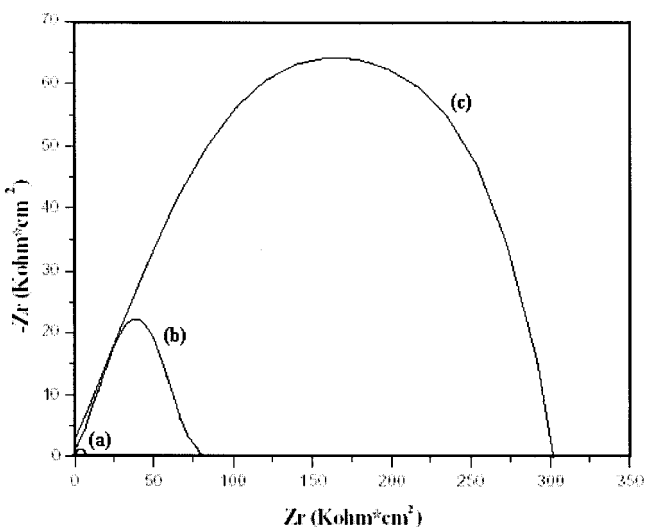

Figure 4 Nyquist plot of three CRS samples in 5 wt % NaCl aqueous solution: (a) bare; (b) P3HT-coated; (c) CL05-coated.

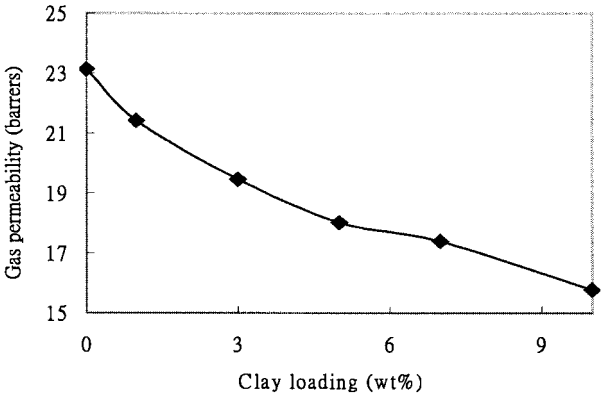

Figure 5 Permeability of O_2 as a function of the MMT clay content in the P3HT–clay nanocomposite membranes.

corrosion products of P3HT and PCN samples showed a grayish oxide layer formed on the top of the exposed CRS surface, similar to what was reported by Wessling with polyaniline-dispersion coatings on steel.[28] The grayish oxide layer might be associated with the redox catalytic property of P3HT. The further enhanced anticorrosion of PCN materials compared to bulk P3HT might have resulted from dispersing silicate nanolayers of clay in the P3HT matrix to increase the O_2 gas-barrier properties of the polymer,[19–21] which is discussed in the following section.

Gas-barrier properties and mechanical strength of membranes

Compared to bulk P3HT, the PCN membrane consisting of 5 wt % clay loading at a comparable permeability value exhibited about a 25% reduction in O_2 permeability, as shown in Figure 5. This resulted from the clay platelets that were dispersed in the composite to increase the tortuousity of the diffusion pathway of the oxygen gas. As the loading of MMT clay increased, the gas barrier of the PCN materials became higher. Figure 6 shows a typical DMA scan of the membrane, in which the storage modulus (E') and loss modulus (E'') were determined in the temperature range of −50 to 100°C at a heating rate of 5°C/min under a nitrogen atmosphere. At the temperature of −50°C, the storage modulus of the membrane with 3 wt % clay loading ($E' = 1.78 \times 10^9$ Pa) [Fig. 6 (A), curve (b)] and 10 wt % clay loading ($E' = 1.04 \times 10^9$ Pa) [Fig. 6 (A), curve (c)] were lower than that of P3HT ($E' = 2.01 \times 10^9$ Pa) [Fig. 6(A), curve (a)]. This might be attributed to the observed large decrease in the crystallinity and molecular weight of P3HT in PCN materials, which led to a significant decrease in mechanical strength. Furthermore, the loss modulus (E'') of P3HT showed a maximum at −5.7°C, which should be involved with the glass transition temperature (T_g) of the bulk polymer,[29] as shown in Figure 6(B). As the loading of MMT

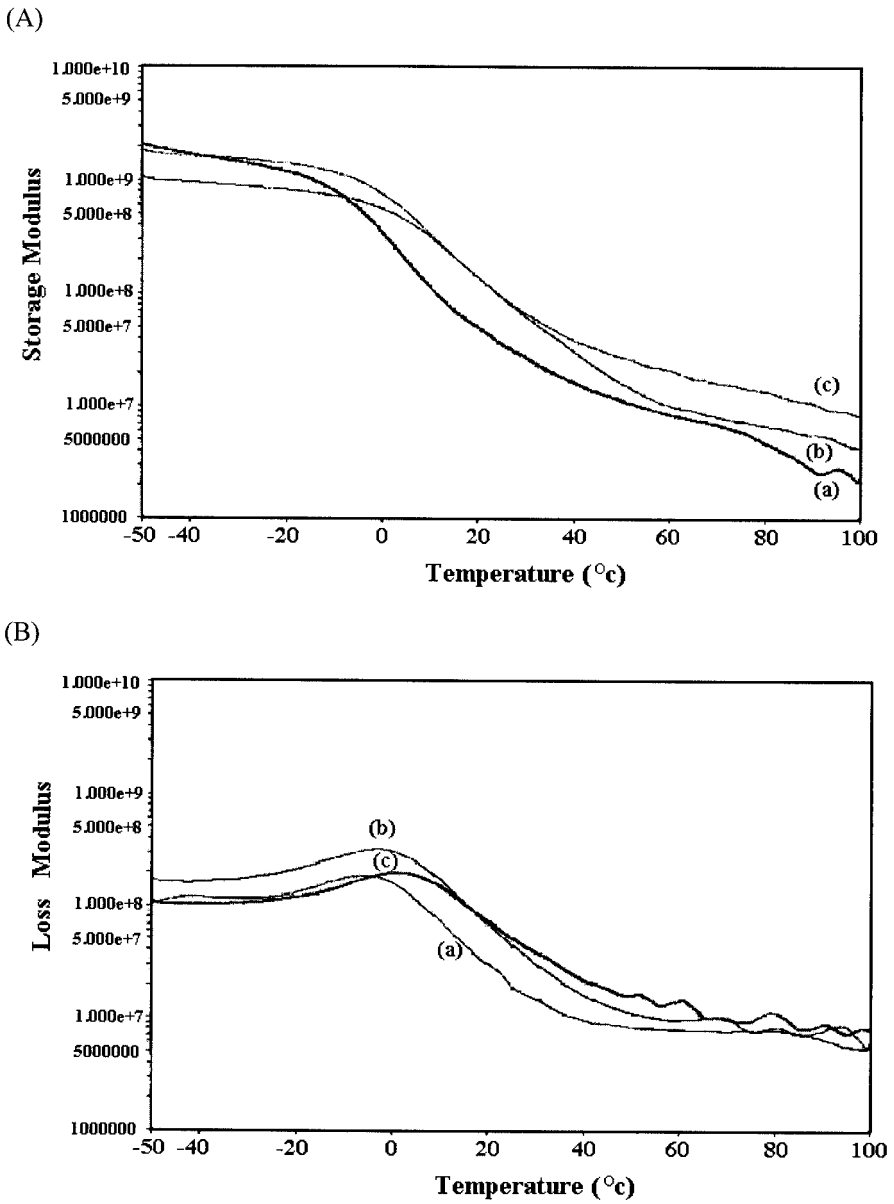

Figure 6 Relationship between modulus and temperature as obtained from DMA measurements on the membranes of (a) P3HT, (b) CL03, and (c) CL10. (A) storage modulus (E'); (B) loss modulus (E'').

clay increased further, the T_g of the PCN materials became higher.

M_w determination of extracted and bulk P3HT

Molecular weights of the various polymer samples recovered from the nanolayers of MMT clays were obtained by GPC analyses with THF as an eluant. The GPC elution pattern of the THF-soluble component displayed a single peak, corresponding to a specific molecular weight value, as summarized in Table II. The molecular weights of P3HT extracted from the PCN materials (to CL05) were found to be slightly lower than that of the bulk P3HT, indicating the structurally restricted polymerization conditions in the intragallery region of the MMT clay[13] and/or the nature of clay oligomer interactions, such as adsorption, during the polymerization reaction.

TABLE II
Molecular Weights of Bulk and Extracted P3HT

Material	M_w	M_n	Polydispersity
Bulk polymer	127,000	24,400	5.2
CL01	119,000	16,700	7.1
CL03	94,000	13,000	7.2
CL05	91,000	12,900	7.1
CL07	89,000	12,500	7.1
CL10	88,000	11,800	7.4

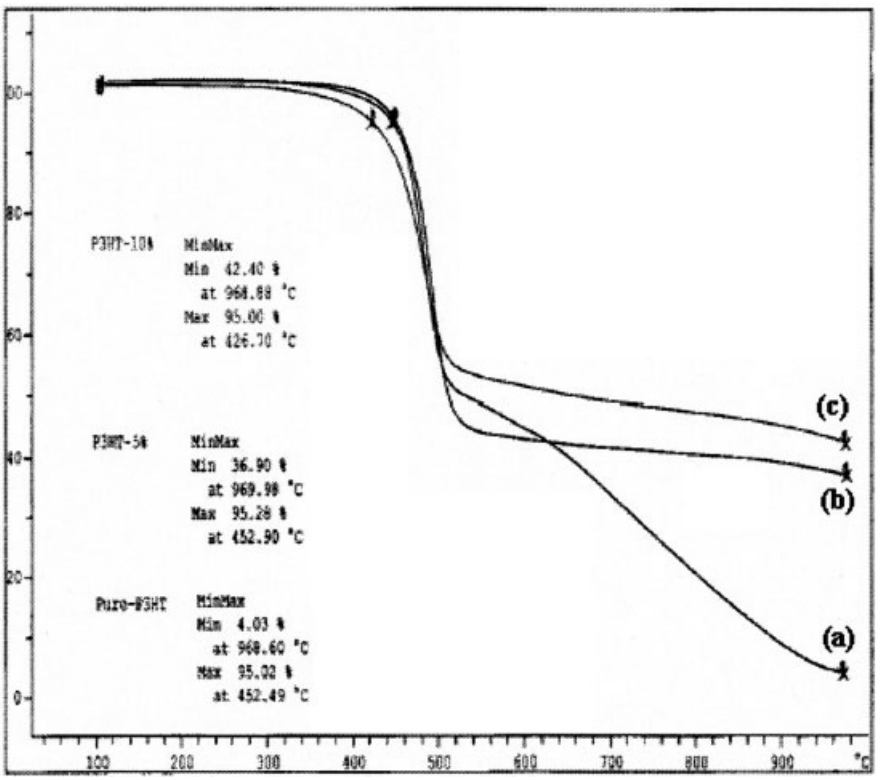

Figure 7 TGA curves of (a) P3HT, (b) CL05, and (c) CL10.

Thermal stability, flammability properties, and electrical conductivity of fine powders

Figure 7 shows typical TGA thermograms of weight loss as a function of the temperature for P3HT and the PCN materials, as measured under an air atmosphere. Generally, there appeared to be one stage of weight loss starting at 100°C and ending at 1000°C, which might correspond to the structural decomposition of the polymers. The decomposition temperature of the PCN materials was shifted toward the slightly lower temperature range than that of P3HT, which may be associated with the obvious decrease in the molecular weight of extracted P3HT in the PCN materials.[19] The residues of the PCN materials determined from TGA (experimental value) were found to be significantly higher than were the values calculated from the feed composition, as shown in Table I. The calculated inorganic contents tend to be lower than those of the experimental values, probably because of the formation of silicate-rich char to enhance the flame retardancy of the materials. The flammability properties of the obtained P3HT and PCN materials were further examined by measuring the LOI value of the materials. A significant increase in the LOI value was observed when the MMT clay was effectively dispersed in the polymer matrix, as shown in Table I. This indicates that the incorporation of MMT into the polymer matrix efficiently increased the flame retardancy of the polymers. It was also noteworthy that the LOI values increased with an increase in the MMT content of the polymers. A flammability reduction mechanism was reported by Gilman et al.[30] The multilayered carbonaceous-silicate structure was found to improve the performance of the char through structural reinforcement. This silicate-rich char might function as an excellent insulator and mass-transport barrier, slowing the escape of the volatile products generated when the polymer decomposed.[31] For the electronic property studies, the electrical conductivity of all the PCN materials in the form of powder-pressed pellets were found to be smaller than that of pristine P3HT based on the four-point probe measurements, as listed in Table I. This was expected because the MMT component was not electrically conductive and the incorporation of MMT clay into the P3HT matrix contributed to the destruction of the polymer crystallinity and lowering of the molecular weight, reflecting a decreased electrical conductivity.

CONCLUSIONS

In this article, we presented the first preparation of P3HT–clay nanocomposite materials. The as-synthesized PCN materials were subsequently characterized by FTIR spectroscopy, WAXRD, and TEM.

PCN materials in the form of coatings with low clay loading on CRS coupons exhibited better anticorro-

sion compared to bulk P3HT on the basis of a series of electrochemical corrosion measurements in saline. PCN materials in the form of a membrane incorporating a small amount of dispersing clay platelets were found to be superior in the gas barrier over those of bulk P3HT based on a series of O_2 gas-permeability measurements. The molecular weights of P3HT in the PCN materials were found to be slightly lower than those of bulk P3HT determined by GPC with THF as the eluant. The decomposition temperature of PCN materials was shifted to a slightly lower temperature range than that of P3HT, which may be associated with the obvious decrease in the molecular weight of the extracted P3HT in the PCN materials. The incorporation of nanolayers of MMT clay in the P3HT matrix led to a decrease in the storage modulus (E') and an increase in glass transition temperature (T_g), in the form of a membrane, based on the DMA studies. This might be attributed to the significantly decreased crystallinity and molecular weight of P3HT formed in the MMT clay. A significant increase in the LOI was observed when MMT was effectively dispersed in the polymer matrix. This indicated that the incorporation of MMT into the polymer matrix efficiently increased the flame retardancy of the polymers. It was also noteworthy that the LOI values increased with an increase in the MMT content of the polymers. Dispersed nanolayers of MMT clays in P3HT led to a significant decrease of electrical conductivity based on the four-point probe technique measurements.

The financial support of this research by the NSC (92-2113-M-033-004) is gratefully acknowledged by the authors.

References

1. Thompson, K. G.; Bryan, C. J.; Benicewicz, B. C.; Wrobleski, D. A. Polym Prepr 1994, 35, 265.
2. Wei, Y.; Wang, J.; Jia, X.; Yeh, J.-M.; Spellane, P. Polymer 1995, 36, 4535.
3. Musselman, I. H.; Li, L.; Washmon, L.; Varadarajan, D.; Riley, S. J.; Hmyene, M.; Ferraris, J. P.; Balkus, K. J., Jr. J Membr Sci 1999, 152, 1.
4. Teng, M.-Y.; Lee, K.-R.; Liaw, D.-J.; Lai, J.-Y. Polymer 2000, 41, 2047.
5. Pinnavaia, T. J. Science 1983, 220, 365.
6. Messersmith, P. B.; Ginnelis, E. P. J Polym Sci Part A Polym Chem 1995, 33, 1047.
7. Lan, T.; Kaviratna, P. D.; Pinnavaia, T. J Chem Mater 1994, 6, 573.
8. Kojima, Y.; Fukumori, K.; Usuki, A.; Okada, ; Kurauchi, T. Mater Sci Lett 1993, 12, 889.
9. Tyan, H.-L.; Liu, Y.-C.; Wei, K.-H. Chem Mater 1999, 11, 1942.
10. Wang, Z.; Pinnavaia, T. J. Chem Mater 1998, 10, 3769.
11. Gilman, J. W.; Jackson, C. L.; Morgan, A. B.; Hayyis, R., Jr.; Manias, E.; Giannelis, E. P.; Wuthenow, M.; Hilton, D.; Phillips, S. H. Chem Mater 2000, 12, 1866.
12. Biswas, M.; Ray, S. S. J Appl Polym Sci 2000, 77, 2948.
13. Wu, C.-G.; DeGroot, D. C.; Marcy, H. O.; Schindler, J. L.; Kannewurf, C. R.; Liu, Y.-J.; Hirpo, W.; Kanatzidis, M. G. Chem Mater 1996, 8, 1992.
14. Wang, L.; Brazis, P.; Rocci, M.; Kannewurf, C. R.; Kanatzidis, M. G. Chem Mater 1998, 10, 3298.
15. Chao, K.-J.; Ho, S.-Y.; Chang, T.-C. U.S. Patent 5 340 500, 1994.
16. Giannelis, E.; Mehrota, V. U.S. Patent 5 032 547, 1991.
17. Choi, H. J.; Kim, J. W.; Kim, S. G.; Kim, B. H.; Joo, J. Polym Mater Sci Eng 2000, 82, 245.
18. Wu, Q.; Xue, Z.; Qi, Z.; Wang, F. Polymer 2000, 41, 2029.
19. Yeh, J.-M.; Liou, S.-J.; Lai, C.-Y.; Wu, P.-C.; Tsai, T.-Y. Chem Mater 2001, 13, 1131.
20. Yeh, J.-M.; Liou, S.-J.; Lin, C.-Y.; Cheng, C.-Y.; Chang, Y.-W.; Lee, K.-R. Chem Mater 2002, 14, 154.
21. Yeh, J. M.; Chen, C. L.; Chen, Y. C.; Ma, C. Y.; Lee, K.-R.; Wei, Y.; Li, S. Polymer 2002, 43, 2729.
22. Akorna, G.; Ugi, I. Angew Chem Int Ed 1977, 16, 259.
23. Nair, C. P. R.; Glouet, G.; Guilbert, Y. Polym Degrad Stab 1989, 26, 305.
24. Hotta, S.; Rughooprth, S. D.; Heeger, A. J. Synth Met 1987, 22, 79.
25. Kang, E. T.; Tan, K. L.; Liaw, D. J.; Chiang, H. H. J Mater Sci 1996, 31, 1295.
26. Yano, K.; Usuki, A.; Okada, A. J Polym Sci Polym Chem Ed 1997, 35, 2289.
27. Yu, Y.-H.; Lin, C.-Y.; Yeh, J.-M.; Lin, W.-H. Polymer 2003, 44, 3553.
28. Wessling, B. Adv Mater 1994, 6, 226.
29. Wei, Y.; Jang, G.-Y.; Hsueh, K.-F.; Scherr, E. M.; MacDiarmid, A. G.; Epstein, A. J. Polymer 1992, 33, 314.
30. (a) Gilman, J. W.; Kashiwagi, T.; Brown, J. E. T.; Lomakin, S.; Giannelis, E. P.; Manias, E. In Proceedings of 43rd International SAMPE Symposium and Exhibition, May 1998; p 1053. (b) Gilman, J. W.; Kashiwagi, T.; Nyden, M.; Brown, J. E. T.; Jackson, C. L.; Lomakin, S.; Giannelis, E. P.; Manias, E. Chemistry and Technology of Polymer Additives; Blackwell: Oxford, 1999; p 249.
31. Gilman, J. W. Appl Clay Sci 1999, 15, 31.